Probability Density Function for Adsorption Energies over Time on Heterogeneous Surfaces by Inverse Gas Chromatography

N. A. Katsanos* and E. Iliopoulou

Physical Chemistry Laboratory, University of Patras, 265 00 Patras, Greece

F. Roubani-Kalantzopoulou and E. Kalogirou

Department of Chemical Engineering, National Technical University, 157 80 Zografou, Greece

Received: August 7, 1999

The inverse gas chromatographic method of reversed-flow gas chromatography is extended to the measurement of the probability density function $f(\epsilon)$ for the adsorption energies on heterogeneous surfaces, as a function of the experimental time. The values of $f(\epsilon)$ are not found from the solution of an integral equation, but by their direct calculation from experimental data in a very simple way. The method is applied to the adsorption of $(CH_3)_2S$ on $CaCO_3$ and $CaCO_3$ + C, in the presence and in the absence of NO_2, at two temperatures around 303 and 323 K. The kinetic physicochemical parameters for the adsorption/desorption phenomena are also calculated for the above systems. The normalization of the $f(\epsilon)$ found, with respect to time, is easily done.

Introduction

The inverse gas chromatographic tool of reversed-flow gas chromatography (RF-GC) was recently applied[1] to measure the time distribution of adsorption energies, ϵ, the local monolayer capacities, c^*_{max}, and the local isotherms, $\theta_i(p,T,\epsilon)$ for some probe gases on heterogeneous solid surfaces in the presence of nitrogen as carrier gas. The method does not depend on analytical or numerical solutions of the classical integral equation

$$\Theta(p, T) = \int_0^\infty \theta_i(p,T,\epsilon)\, f(\epsilon)\, d\epsilon \qquad (1)$$

where $\Theta(p,T)$ is the overall experimental adsorption isotherm and $f(\epsilon)$ is the probability density function for the adsorption energies, but on a time function of the chromatographic peaks obtained by short flow reversals of the carrier gas:

$$H^{1/M} = \sum_{i=1}^{4} A_i \exp(B_i t) \qquad (2)$$

where H is the peak height, M is the response factor of the detector, A_i is the preexponential factors, and B_i is the exponential coefficients of time t, when flow reversals were made. For convenience, Figure 1 of the previous publication[1] is repeated here. The calculation of B_i values from the experimental pairs H, t and their physical content has been reported earlier.[2,3] The relevant mathematical model was based on two mass balances of the probe gaseous concentrations, the rate of change of the adsorbed concentration on the heterogeneous solid surface, and an isotherm for the local adsorbed equilibrium concentration on the solid. The term "local" means with respect to time, i.e., involving only a limited collection of adsorption sites active at time t.

* To whom correspondence should be addressed: FAX number: +30-61-997110. INTERNET address: Katsanos@otenet.gr.

The necessary relations for calculating from eq 2 the values of ϵ, c^*_{max} and θ_i for the adsorption of gases on heterogeneous surfaces as a function of time have been derived[1] by combining eq 2 with the Jovanovic isotherm model:

$$\theta(p,T,\epsilon) = 1 - \exp(-Kp) \qquad (3)$$

where

$$K = K^0(T) \exp(\epsilon/RT) \qquad (4)$$

R being the gas constant and K^0 being given by eq 9 of ref 1.

Four auxiliary relations, involving A_i, B_i, and t of eq 2, give as functions of them the gaseous concentration c_y (mol/cm^3) of the adsorbate A (eq 4 of ref 1), its local adsorbed equilibrium concentration c^*_s (eq 5 of ref 1), and the two partial derivatives $\partial c^*_s/\partial c_y$ and $\partial^2 c^*_s/\partial c_y^2$ (eqs 6 and 14, respectively, of ref 1).

It has been shown before (eq 13 of ref 1) that the ratio of the last two partial derivatives, equals $-KRT$, where K is Langmuir's constant of eq 4.

Substituting in the above ratio of the two partial derivatives the right-hand sides of eqs 6 and 14 of ref 1, one finds, in view also of eq 4,

$$KRT = RTK^0 \exp(\epsilon/RT) = \frac{gD_1}{\upsilon L_1}\left\{\frac{\sum_i A_i B_i^2 \exp(B_i t)}{[\sum_i A_i B_i \exp(B_i t)]^2} - \frac{1}{\sum_i A_i \exp(B_i t)}\right\} \qquad (5)$$

where υ (cm/s) is the corrected linear flow velocity of the carrier gas, L_1 (cm) is the length of section z of the diffusion column (cf. Figure 1), g is the calibration factor of the chromatographic detector in cm (peak height)/mol cm^{-3}, and D_1 (cm^2/s) is the diffusion coefficient of A in section z of the diffusion column.

10.1021/jp992788h CCC: $18.00
Published on Web 10/30/1999

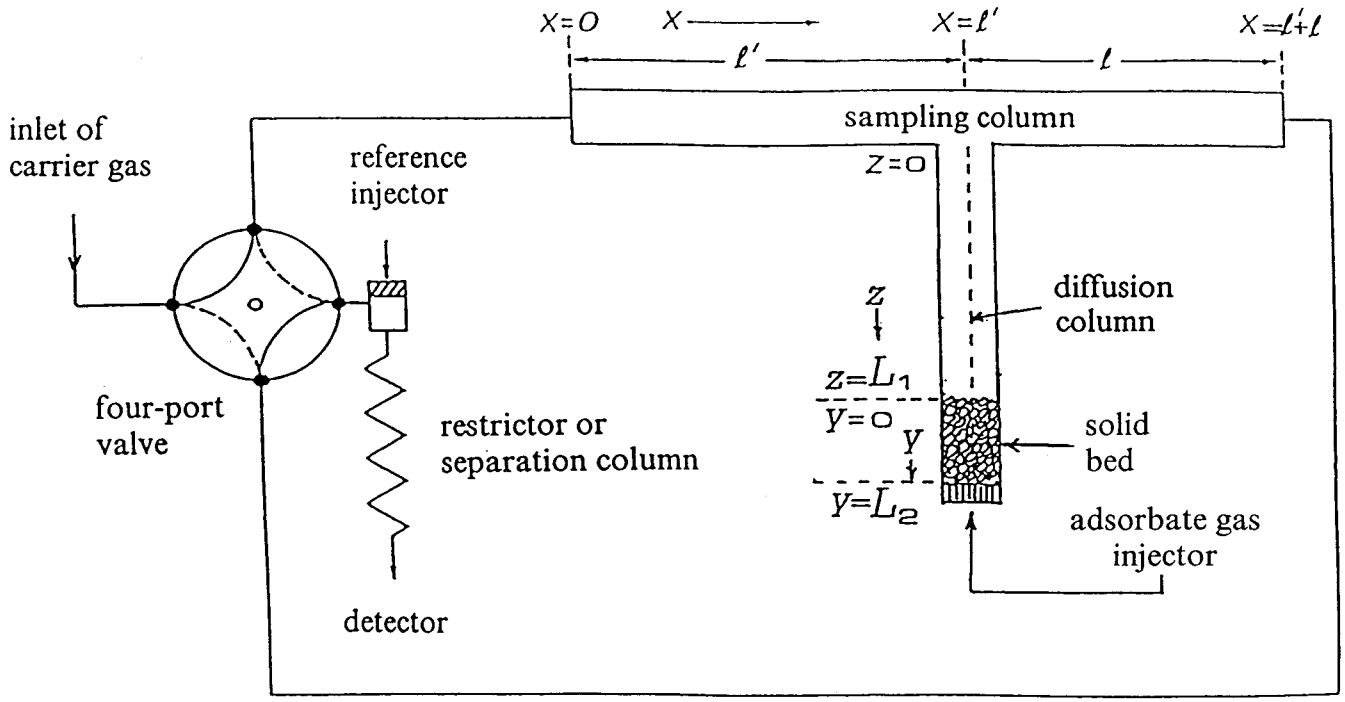

Figure 1. Schematic representation of the columns and gas connections showing the principle for using the reversed-flow technique as an inverse gas chromatographic tool.

The relation for calculating ϵ (kJ/mol) from experimental data follows from the left part of eq 5, i.e.

$$\epsilon = RT\,[\ln(KRT) - \ln(RT) - \ln K^0] \tag{6}$$

whereas the relation for calculating c^*_{max} (mol/g) and θ_t are

$$c^*_{max} = c^*_s + \frac{\partial c^*_s/\partial c_y}{KRT} \tag{7}$$

$$\theta_t = 1 - \frac{1}{c^*_{max}}\frac{\partial c^*_s/\partial c_y}{KRT} \tag{8}$$

All above calculations are easily carried out by running the PC program in GW-BASIC available as Supporting Information of ref 1.

In the present work the probability density function with respect to the energy, $f(\epsilon)$, over time on a heterogeneous surface is approached, neither by seeking analytical solutions of the integral eq 1 nor by employing numerical solutions and estimation methods, as recently reviewed,[2] but by a direct calculation of $f(\epsilon)$ from experimental data (eq 2) in a relatively simple way.

The new method for finding $f(\epsilon)$ is exemplified by presenting results of dimethyl sulfide vapor adsorbed on pieces of Penteli marble (pure or covered with carbon black), in the absence and presence of gaseous nitrogen dioxide, in a pure nitrogen atmosphere.

Theory

According to Jaroniec and Madey,[4] the probability function $f(\epsilon)$ of eq 1, describing the adsorption energy distribution, is defined as "the derivative of the number of adsorption sites with respect to the adsorption energy". Since the number of adsorption sites is proportional to the local monolayer capacity c^*_{max} of eq 7, one may define $f(\epsilon)$ as

$$f(\epsilon) = \frac{\partial c^*_{max}}{\partial \epsilon} = \frac{\partial c^*_s}{\partial \epsilon} + \frac{\partial^2 c^*_s/\partial c_y \partial \epsilon}{RTK^0 \exp(\epsilon/RT)} - \frac{\partial c^*_s/\partial c_y}{(RT)^2 K^0 \exp(\epsilon/RT)} \tag{9}$$

The far-right-hand side of the above equation was obtained from eq 7 by differentiation with respect to the energy ϵ. It is obvious that $f(\epsilon)$ is an explicit function of energy ϵ, $f(\epsilon)d\epsilon$ giving the probability for adsorption energies in the interval between ϵ and $\epsilon + d\epsilon$.

Since both c^*_{max} and ϵ change with the time of measurement,[1] the simplest way to calculate $f(\epsilon)$ is through the relation

$$f(\epsilon;t) = \frac{\partial c^*_{max}}{\partial \epsilon} = \frac{\partial c^*_{max}/\partial t}{\partial \epsilon/\partial t} \tag{10}$$

In this equation t is a structural parameter and not a random variable. Thus, $f(\epsilon)$ as defined by $\partial c^*_{max}/\partial \epsilon$ above is a function of two independent variables, ϵ and t, but a probability density function of ϵ only.

The numerator of the right-hand side of eq 10 above may be easily found from eq 7, and the denominator from eq 6, simply by differentiation with respect to t:

$$\frac{\partial c^*_{max}}{\partial t} = \frac{\partial c^*_s}{\partial t} + \frac{1}{(KRT)^2}\left[KRT\frac{\partial^2 c^*_s}{\partial c_y \partial t} - \frac{\partial c^*_s}{\partial c_y}\frac{\partial (KRT)}{\partial t}\right] \tag{11}$$

$$\frac{\partial \epsilon}{\partial t} = RT\frac{\partial \ln(KRT)}{\partial t} = \frac{1}{K}\frac{\partial (KRT)}{\partial t} \tag{12}$$

Dividing eq 11 by eq 12, according to eq 10, one obtains

$$f(\epsilon) = \frac{1}{RT}\left[\frac{KRT(\partial c^*_s/\partial t) + \partial^2 c^*_s/\partial c_y \partial t}{\partial (KRT)/\partial t} - \frac{\partial c^*_s/\partial c_y}{KRT}\right] \tag{13}$$

All derivatives with respect to time in the above relation are

explicitly and analytically calculated from relations already given, namely, $\partial c_s^*/\partial t$ from eq 5, of ref 1, $\partial(KRT)/\partial t$ from eq 5, and $\partial^2 c_s^*/\partial c_y \partial t$ from eq 6 of ref 1:

$$\frac{\partial c_s^*}{\partial t} = \frac{M_1}{M_2}\sum_i A_i \exp(B_i t) \tag{14}$$

$$\frac{\partial(KRT)}{\partial t} = M_2\left\{\frac{\sum_i A_i B_i^3 \exp(B_i t)}{[\sum_i A_i B_i \exp(B_i t)]^2} - \frac{2[\sum_i A_i B_i^2 \exp(B_i t)]^2}{[\sum_i A_i B_i \exp(B_i t)]^3} + \frac{\sum_i A_i B_i \exp(B_i t)}{[\sum_i A_i \exp(B_i t)]^2}\right\} \tag{15}$$

$$\frac{\partial^2 c_s^*}{\partial c_y \partial t} = M_1\left\{1 - \frac{[\sum_i A_i \exp(B_i t)][\sum A_i B_i^2 \exp(B_i t)]}{[\sum_i A_i B_i \exp(B_i t)]^2}\right\} \tag{16}$$

where

$$M_1 = \frac{a_y k_1}{a_s} \quad \text{and} \quad M_2 = \frac{gD_1}{\upsilon L_1} \tag{17}$$

a_y (cm^2) is the cross sectional area of the void space in the solid bed, a_s (g/cm) is the amount of solid adsorbent per unit length of bed, and k_1 (s^{-1}) is the adsorption rate constant of A on the surface.

Finally, substitution of eqs 14−16 for the derivatives $\partial c_s^*/\partial t$, $\partial(KRT)/\partial t$ and $\partial^2 c_s^*/\partial c_y \partial t$, respectively, into eq 13, together with eq 5 for KRT and eq 6 of ref 1 for $\partial c_s^*/\partial c_y$ gives $f(\epsilon)$ as an analytic function of the structural parameter t, $f(\epsilon;t)$.

Calculations

As before,[1] the calculations of the physicochemical quantities ϵ, c_y, and $f(\epsilon)$ pertaining to heterogeneous surfaces start from the diffusion band of RF-GC experiments by recording the pairs H, t and calculating the preexponential factors A_1, A_2, A_3, and A_4 and the time coefficients B_1, B_2, B_3, and B_4 of eq 2, together with the rate constant k_1, the calibration factor g, and the diffusion coefficient D_1, as previously reported.[2] The other quantities needed, i.e., υ, a_y, a_s, L_1, R, k, h, T, and m, are known experimentally or they are physical constants from the literature.

Using all above quantities in eqs 9, 4, and 6 of ref 1 and eqs 5, 14, 15, and 16 here, one calculates K^0, c_y, $\partial c_s^*/\partial c_y$, KRT, $\partial c_s^*/\partial t$, $\partial(KRT)/\partial t$, and $\partial^2 c_s^*/\partial c_y \partial t$, respectively. These are then used with eqs 6 and 13 to find the values of ϵ and $f(\epsilon)$, respectively, for any chosen time t, measured from the introduction of the analyte gas A into the solid adsorbent bed.

Instead of the above procedure, one may use the PC program in GW-BASIC available as Supporting Information in the present work to conduct all above calculations and find directly from the experimental pairs H, t the values of c_y, ϵ, and $f(\epsilon)$, together with the adsorption parameter k_1, the desorption rate constant k_{-1}, a possible first-order surface reaction rate constant k_2, the deposition velocity V_d, and the reaction probability γ of the probe gas A on the solid surface, the effective diffusion coeffient D_1 of A into the carrier gas, and the detector calibration factor g. The values M (of eq 2), a_y, a_s, υ, and L_1 needed in the calculations and some other known data are entered into the appropriate INPUT lines of the program, together with the ranges t_1 and t_2 in which c_y, ϵ, and $f(\epsilon)$ are calculated and printed. Equations 9, 4, and 6 of ref 1 and eqs 5, 6, and 13−16 here may also be used with the PC program MATHEMATICA 3 to plot c_y, ϵ, and $f(\epsilon)$ vs t between the two limits of the experimental time with a number of plot points of, e.g., 3000.

Since $f(\epsilon;t)$ is an analytic function of the structural parameter t, it can be easily normalized to unity with respect to time

$$\int_{t_1}^{t_2} f(\epsilon;t)\, dt = 1 \tag{18}$$

by finding the value of the above integral between the two limits t_1 and t_2 of the experimental time and dividing $f(\epsilon;t)$ by the result.

TABLE 1: Time Distribution of the Gaseous Concentration (c_y), the Adsorption Energy (ϵ), and the Probability Density Function [$f(\epsilon)$], for Penteli Marble ($CaCO_3$, $CaCO_3$ + C), after Injecting 2 μL of Liquid $(CH_3)_2S$, at 304.9 and 303.1 K

	$CaCO_3$ at 304.9 K			$CaCO_3$ + C at 303.1 K		
time, min	$10^6 c_y$, mol/cm^3	ϵ, kJ/mol	$10^6 f(\epsilon)$, mol^2/(kJ g)	$10^7 c_y$, mol/cm^3	ϵ, kJ/mol	$10^7 f(\epsilon)$, mol^2/(kJ g)
14				0.382	94.3	0.0144
16				0.996	91.9	0.0843
18	0.129	92.2	0.00929	1.68	90.7	0.209
20	0.405	89.4	0.0906	2.40	90.1	0.375
22	0.677	88.2	0.245	3.13	89.7	0.570
24	0.940	87.6	0.453	3.83	89.5	0.781
26	1.19	87.3	0.694	4.50	89.5	0.996
28	1.42	87.1	0.948	5.13	89.5	1.20
30	1.64	87.1	1.20	5.71	89.6	1.40
32	1.84	87.2	1.43	6.24	89.8	1.57
34	2.02	87.3	1.63	6.71	90.0	1.72
36	2.18	87.6	1.79	7.14	90.3	1.84
38	2.33	87.9	1.91	7.51	90.7	1.93
40	2.45	88.3	1.98	7.84	91.0	1.99
42	2.56	88.8	2.00	8.12	91.5	2.01
44	2.66	89.3	1.96	8.36	92.0	2.00
46	2.73	90.0	1.87	8.57	92.5	1.95
48	2.80	90.8	1.73	8.74	93.2	1.87
50	2.85	91.8	1.53	8.88	93.9	1.75
52	2.89	93.1	1.27	8.99	94.8	1.59
54	2.91	94.8	0.967	9.07	95.8	1.39
56	2.93	97.5	0.608	9.14	97.2	1.15
58	2.94	103.4	0.198	9.18	99.0	0.865
60	2.94	102.3	0.263	9.21	101.8	0.533
62	2.93	97.1	0.774	9.22	108.5	0.150
64	2.92	94.6	1.33	9.22	105.5	0.290
68	2.87	91.7	2.60	9.18	98.4	1.36
72	2.81	89.8	4.07	9.11	95.5	2.74
76	2.73	88.5	5.74	9.01	93.6	4.50
80	2.64	87.5	7.63	8.89	92.2	6.77
84	2.55	86.6	9.76	8.76	91.1	9.69
88	2.45	85.9	12.2	8.62	90.1	13.5
92	2.35	85.2	14.8	8.47	89.1	18.4
96	2.25	84.6	17.8	8.31	88.3	24.8
100	2.15	84.1	21.2	8.16	87.5	33.3
110	1.90	82.9	31.7	7.77	85.5	69.4
120	1.68	81.9	46.1	7.39	83.6	149

Experimental Section

The apparatus and procedure were described elsewhere.[3] Section L_1 (34.5−38.4 cm) was empty of any solid material, while L_2 (8.6−6.8 cm) contained the solid bed. Both L_1 and L_2 were of Pyrex glass with an i.d. of 3.5 mm and heated to the same temperature. The sampling column $l' + l$ (65 + 65 cm) was a stainless steel chromatographic tube of 4 mm i.d. No separation column, but only a restrictor, was used.

TABLE 2: Time Distribution of the Gaseous Concentration (c_y), the Adsorption Energy (ϵ), and the Probability Density Function [$f(\epsilon)$], for Penteli Marble ($CaCO_3$, $CaCO_3$ + C), after Injecting 2 μL of Liquid $(CH_3)_2S$ and 2 μL of Liquid NO_2 at 303 and 301.7 K

	$CaCO_3$ at 303 K			$CaCO_3$ + C at 301.7 K		
time, min	$10^6 c_y$, mol/cm^3	ϵ, kJ/mol	$10^7 f(\epsilon)$, mol^2/(kJ g)	$10^6 c_y$, mol/cm^3	ϵ, kJ/mol	$10^6 f(\epsilon)$, mol^2/(kJ g)
10				0.451	88.4	0.0133
12				1.06	87.0	0.073
14				1.53	86.8	0.148
16	1.04	87.6	0.128	1.88	87.2	0.213
18	1.69	88.1	0.309	2.14	87.9	0.255
20	2.04	90.0	0.363	2.32	88.9	0.268
22	2.19	93.7	0.256	2.45	90.3	0.248
24	2.23	107.9	0.0218	2.52	92.4	0.195
26	2.20	92.8	0.686	2.56	96.1	0.107
28	2.15	83.1	26.0	2.57	106.7	0.0152
30	2.10	92.0	0.920	2.56	95.0	0.175
32	2.07	96.7	0.284	2.53	91.8	0.377
34	2.06	102.7	0.0815	2.49	89.8	0.629
36	2.08	94.2	0.439	2.43	88.4	0.947
38	2.13	91.0	0.901	2.38	87.2	1.35
40	2.21	88.8	1.61	2.32	86.2	1.89
42	2.31	86.9	2.88	2.25	85.2	2.64
44	2.44	84.9	5.60	2.19	84.2	3.76
46	2.58	82.4	14.4	2.12	83.1	5.62
48	2.73	74.4	349	2.06	81.8	9.36
50	2.90	81.7	19.7	2.00	79.8	20.7
52	3.07	83.0	12.1	1.94	69.8	1130
54	3.24	83.7	9.57	1.88	79.5	23.5
56	3.41	84.2	8.38	1.82	81.0	12.8
58	3.58	84.6	7.71	1.76	81.9	9.18
60	3.74	84.9	7.27	1.71	82.5	7.40
64	4.04	85.6	6.70	1.61	83.2	5.67
68	4.31	86.3	6.21	1.52	83.7	4.88
72	4.53	87.2	5.65	1.44	83.9	4.49
76	4.71	88.3	4.94	1.36	84.1	4.31
80	4.84	89.7	4.04	1.29	84.2	4.29
84	4.93	91.7	2.93	1.23	84.3	4.38
88	4.99	95.1	1.59	1.17	84.2	4.56
90	5.00	98.5	0.842	1.14	84.2	4.69
92	5.00	114.7	0.0351	1.11	84.1	4.84
96	4.99	95.3	1.75	1.06	84.0	5.22
100	4.95	91.8	3.75	1.02	83.8	5.70
110	4.75	87.7	9.72			
120	4.46	85.5	17.1			
130	4.13	84.1	25.9			
140	3.78	82.9	36.5			
150	3.43	82.0	49.1			

The $CaCO_3$ was a Penteli marble (Greece), its analysis being given before.[5] It was ground to small pieces of 10−30 mesh, 0.6−1.25 g of which was placed in section L_2 of the apparatus. The $CaCO_3$ + C material was prepared by shaking the above pieces of $CaCO_3$ with 0.13 g of carbon black powder obtained from an automobile exhaust pipe. After sieving the resulted mixture, the 10−30 mesh fraction was retained and 1.26 g was used.

The $(CH_3)_2S$, being the main probe gas, was a product of Fluka (puriss), while NO_2 was prepared in laboratory scale by heating $Pb(NO_3)_2$ of analytical grade at atmospheric pressure and collected under cooling with liquid nitrogen, in the absence of moisture.

The carrier gas was nitrogen (99.99%) from Linde (Athens, Greece), dried by silica gel, with a flow rate of 22 cm^3/min.

The probe gases were introduced through the injector of Figure 1 as liquids (2 μL). The second adsorbate (NO_2) was injected 30 s after the first [$(CH_3)_2S$].

Following the appearance of the continuously rising concentration−time curve in the flame ionization detector of a Shimadzu 14 chromatograph, the flow-reversing procedure of the carrier gas was started, lasting 10−20 s for each reversal, which is shorter than the gas hold-up time in both column sections l' and l. The narrow fairly symmetrical sample peaks created by the flow reversals were recorded, and their height H or the area under the curve was calculated and printed, together with the corresponding time t, by a C-R6A Shimadzu Chromatopac.

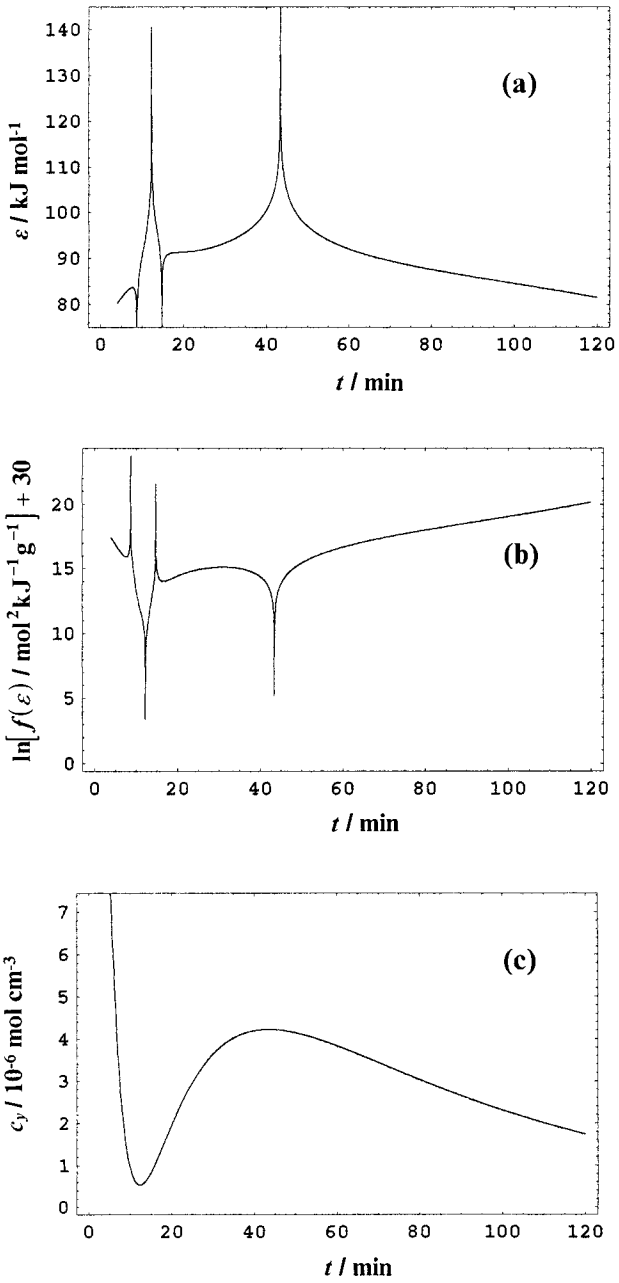

Figure 2. Plots of adsorption energy (a), probability density function (b), and gaseous concentration (c), as a function of experimental time, at 323 K, for the system $(CH_3)_2S/CaCO_3$ in a nitrogen atmosphere.

By entering the pair values of H, t into the 3000−3040 DATA lines of the GW-BASIC program given in the Supporting Information here, together with the other unknown quantities in the INPUT lines 190−350, the physicochemical parameters and functions exposed and defined by eqs 6 and 13 of the previous sections and eq 4 of ref 1 are calculated and printed.

Results and Discussion

The method described in the present work to measure directly from experimental data not only adsorption energies, local

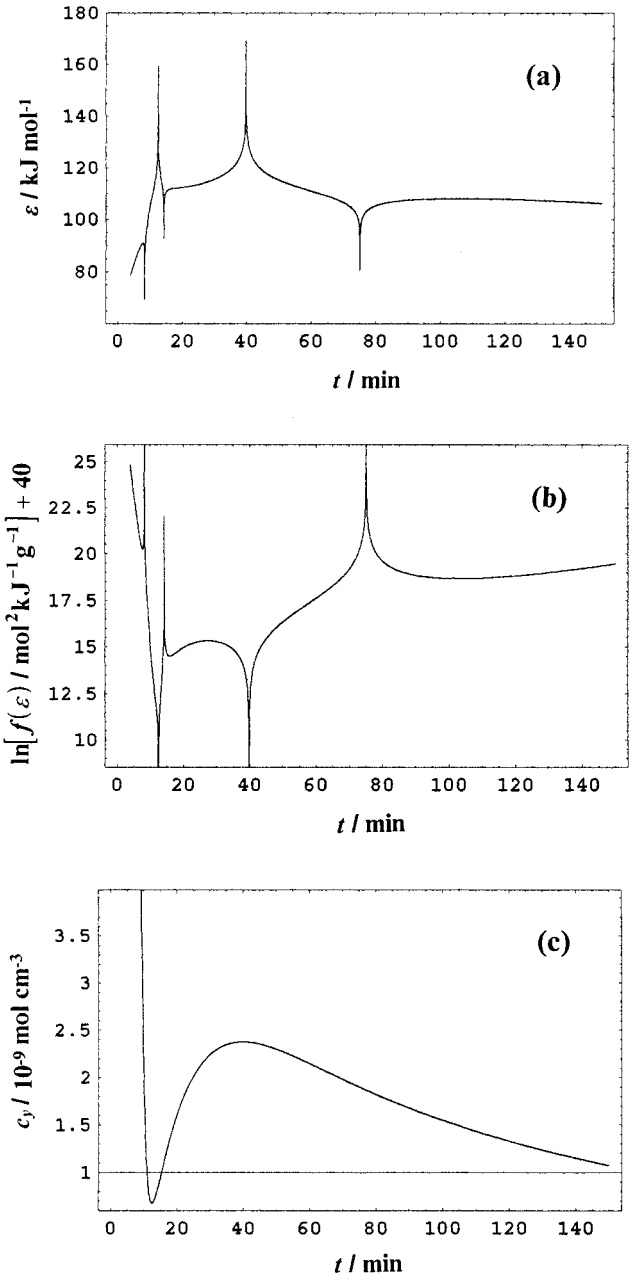

Figure 3. Plots of adsorption energy (a), probability density function (b), and gaseous concentration (c), as a function of experimental time, at 323.2 K, for the system $(CH_3)_2S/CaCO_3$ + C in a nitrogen atmosphere.

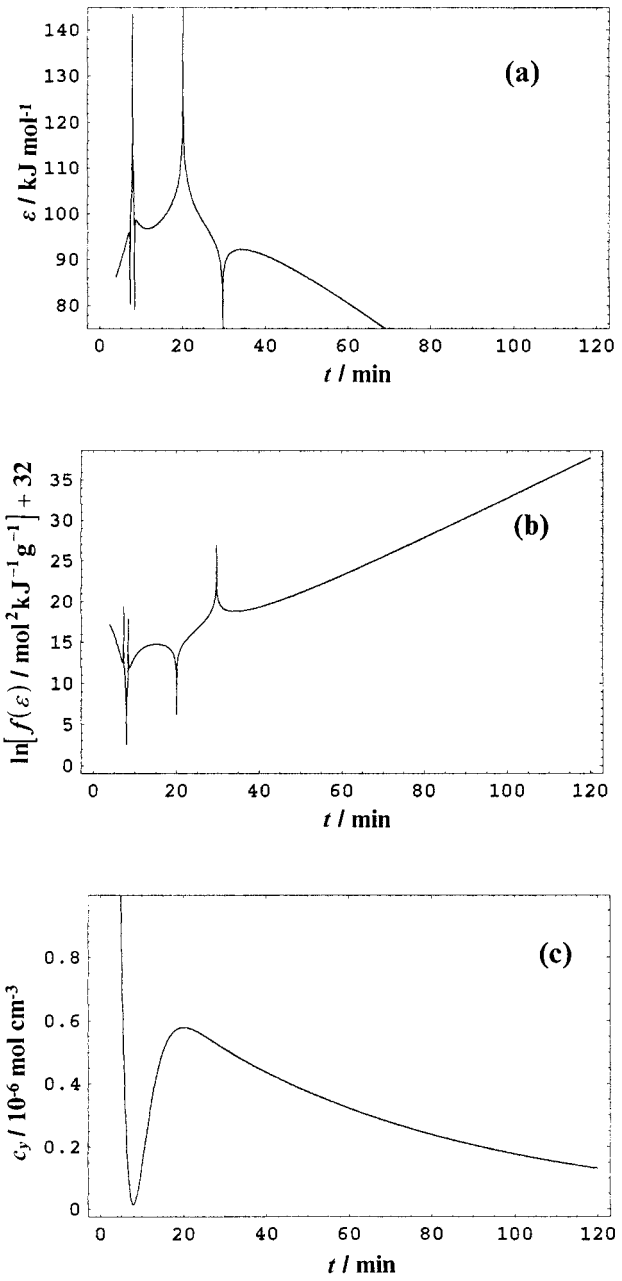

Figure 4. Plots of adsorption energy (a), probability density function (b), and gaseous concentration (c), as a function of experimental time, at 323 K, for the system $(CH_3)_2S$ + $NO_2/CaCO_3$ in a nitrogen atmosphere.

monolayer capacities, and local adsorption isotherms, as previously described,[1] but also the probability density function for the adsorption energies as distributed over experimental time has been applied by using dimethyl sulfide and nitrogen dioxide as probe gases and Penteli marble as the solid adsorbent. The reason for choosing dimethyl sulfide as the main probe gas is that it is emitted by oceanic phytoplankton and constitutes the major natural source of sulfur in the troposphere. Nitrogen dioxide was chosen to see whether this well-known air pollutant in cities has any synergistic effect on the adsorption properties measured. As regards the solid, it is well-known that most Greek cultural heritage objects in the Acropolis of Athens and elsewhere have been constructed with Penteli marble, and adsorption properties such as those described here may throw some light on the mechanism of deterioration of art pieces by air pollutants. Needless to say that carbon black from the exhaust pipes of cars is one of the main kinds of airborne particles in cities, being deposited onto clean solid surfaces, and therefore their effect on adsorption properties of marble is interesting.

Tables 1 and 2 list the values of the gaseous concentration c_y of $(CH_3)_2S$, its adsorption energy ϵ on $CaCO_3$ or $CaCO_3$ + C, and the corresponding probability density function $f(\epsilon)$, in the presence or absence of NO_2, at temperatures 301.7−304.9 K, as functions of various experimental times. The results with similar systems at a higher temperature (323 K) are presented as functions of time, using 3000 plot points. The same plots can be constructed with the systems of Tables 1 and 2.

The appearance of the function $c_y = f(t)$ in Figures 2c−4 c is not typical for the so-called diffusion band of the RF-GC method, where it usually increases initially, passes through a maximum, and then declines with time. Here, this is preceded by a steep falling part related to a peak of high adsorption energy and a low value in the probability density function. These are

not observed at the lower temperatures of 301.7−304.9 K, as Tables 1 and 2 show.

The characteristics common to all regions of c_y are the minima in $f(\epsilon)$ coinciding with the maxima in ϵ. The presence of carbon particles on the surface of $CaCO_3$ and of NO_2 in the gas phase have noticeable effects on ϵ and $f(\epsilon)$.

As pointed out in a previous publication,[1] the gas molecules at time t are not assumed to be exclusively adsorbed on sites i all of the same energy ϵ_i, Figures 2a−4a showing the sweeping effect of the dynamic and changing with time procedure on collection of sites being active at time t and having a mean adsorption energy ϵ. The maxima and minima in the function $\epsilon = g(t)$ represent rather transition adsoption energies before their final leveling off with time.

The functions $f(\epsilon)$ given in Tables 1 and 2 and Figures 2b−4b are unnormalized, but they can be normalized with respect to time, as mentioned in the Calculations, quite easily. For example, the integral of eq 18 for the system of Figure 3 was calculated with three choices of the time period and found to be

$$1.8294 \times 10^{-3} \quad \text{for} \quad t_1 = 0 \quad \text{and} \quad t_2 = 120 \text{ min}$$

$$1.8316 \times 10^{-3} \quad \text{for} \quad t_1 = 0 \quad \text{and} \quad t_2 = 150 \text{ min}$$

$$1.8326 \times 10^{-3} \quad \text{for} \quad t_1 = 0 \quad \text{and} \quad t_2 = 200 \text{ min}$$

Therefore, the normalizing factor in this case is 546.6, 546.0, and 545.7, respectively.

The kinetic physicochemical quantities for the adsorption phenomenon, k_1, k_{-1}, and k_2 have been calculated by the same PC program given in the Supporting Information and are collected in Table 3.

TABLE 3: Adsorption Parameter (k_1), Desorption Rate Constant (k_{-1}), and Surface Reaction Rate Constant (k_2) for $(CH_3)_2S$ Adsorbed on $CaCO_3$ and $CaCO_3$ + C in the Presence and in the Absence of NO_2

system	temp, K	NO_2	10^3k_1, s^{-1}	10^4k_{-1}, s^{-1}	10^3k_2, s^{-1}
$CaCO_3$	304.9	no	7.23	1.00	2.48
$CaCO_3$ + C	303.1	no	3.01	1.77	0.187
$CaCO_3$	303	yes	0.772	12.4	1.25
$CaCO_3$ + C	301.7	yes	3.42	4.37	0.0279
$CaCO_3$ + C	323.2	no	1.87	177	-
$CaCO_3$	323	yes	2.55	92.3	1.81
$CaCO_3$	323	no	1.27	10.8	0.834

Acknowledgment. The help of Prof. S. Kourouklis as regards probability density functions and the technical help of Miss A. Malliori are gratefully acknowledged by the authors.

Supporting Information Available: The PC program in GW-BASIC, for calculating directly from the experimental pairs H, t the various physicochemical quantities is available free of charge via the Internet at http://pubs.acs.org.

References and Notes

(1) Katsanos, N. A.; Arvanitopoulou, E.; Roubani-Kalantzopoulou, F.; Kalantzopoulos, A. *J. Phys. Chem. B* **1999**, *103*, 1152.

(2) Katsanos, N. A.; Thede, R.; Roubani-Kalantzopoulou, F. *J. Chromatogr. A* **1998**, *795*, 133.

(3) Abatzoglou, Ch.; Iliopoulou, E.; Katsanos, N. A.; Roubani-Kalantzopoulou, F.; Kalantzopoulos, A. *J. Chromatogr. A* **1997**, *775*, 211.

(4) Jaroniec, M.; Madey, R. *Physical Adsorption on Heterogeneous Solids*; Elsevier: Amsterdam, 1988; p 13.

(5) Katsanos, N. A.; Karaiskakis, G. *J. Chromatogr.* **1987**, *395*, 423.